

Bubble wall velocity in cosmological phase transitions: electroweak baryogenesis and gravitational waves

Marek Lewicki

University of Warsaw

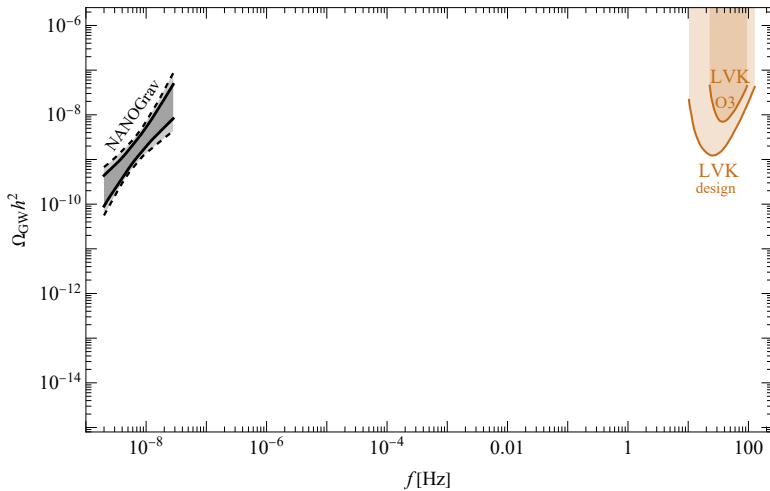
CERN Cosmo Coffee seminar, 22 V 2024

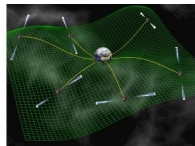
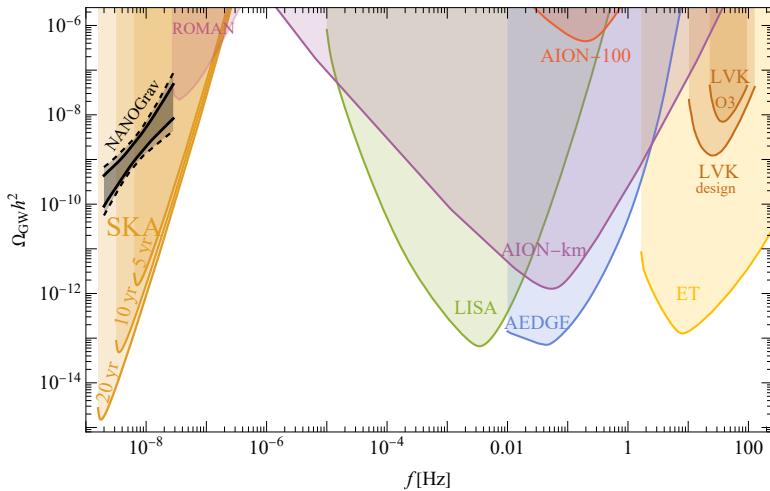
POLSKIE POWROTY
POLISH RETURNS



UNIVERSITY
OF WARSAW

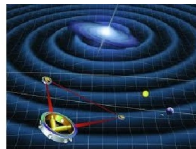






Pulsar Timing

[David Champion/NASA/JPL]



LISA
[wiki/Laser_Interferometer_Space_Antenna](https://en.wikipedia.org/wiki/Laser_Interferometer_Space_Antenna)

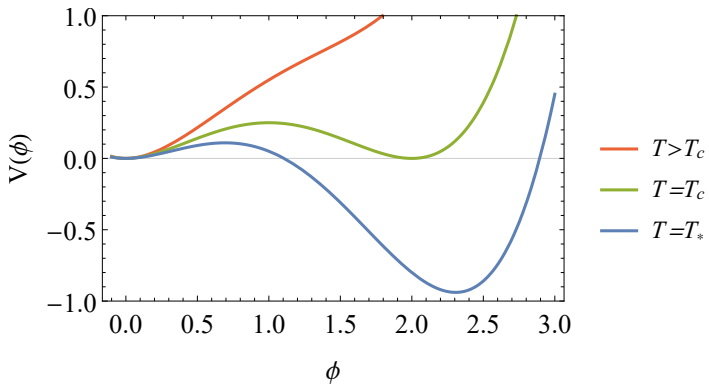


Einstein Telescope
www.et-gw.eu

First Order Phase Transition

- Simple high temperature expansion

$$V(\phi, T) = \frac{g_m^2}{24} (T^2 - T_0^2) \phi^2 - \frac{g_m}{12\pi} T \phi^3 + \lambda \phi^4, \quad T_0^2 > 0$$



First Order Phase Transition: bubble nucleation

- Temperature corrections to the potential

$$V(\phi, T) = \frac{g_m^2}{24} (T^2 - T_0^2) \phi^2 - \frac{g_m}{12\pi} T \phi^3 + \lambda \phi^4$$

- EOM \rightarrow bubble profile

$$\frac{d^2\phi}{dr^2} + \frac{2}{r} \frac{d\phi}{dr} - \frac{\partial V(\phi, T)}{\partial \phi} = 0,$$

$$\phi(r \rightarrow \infty) = 0 \quad \text{and} \quad \dot{\phi}(r=0) = 0.$$

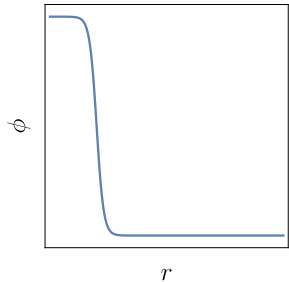
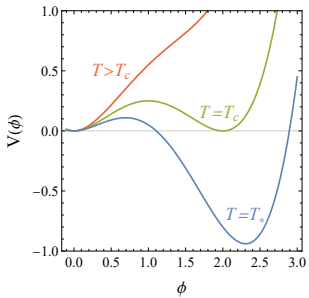
- $\mathcal{O}(3)$ symmetric action

$$S_3(T) = 4\pi \int dr r^2 \left[\frac{1}{2} \left(\frac{d\phi}{dr} \right)^2 + V(\phi, T) \right].$$

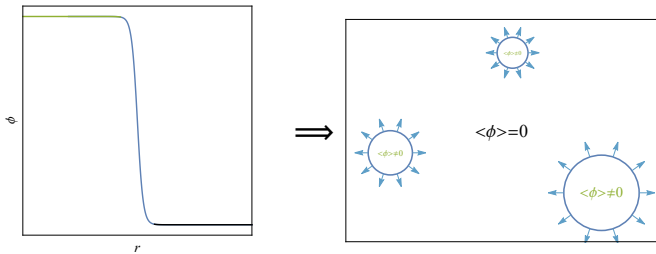
- nucleation temperature

$$\frac{\Gamma}{H^4} \approx \left(\frac{T}{H} \right)^4 \exp \left(- \frac{S_3(T)}{T} \right) \approx 1$$

Linde '81 '83



Phase transition parameters



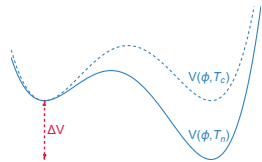
- Strength of the transition

$$\alpha \approx \left. \frac{\Delta V - \frac{T}{4} \frac{\partial \Delta V}{\partial T}}{\rho_R} \right|_{T=T_*}, \quad \Delta V = V_f - V_t$$

- Characteristic scale

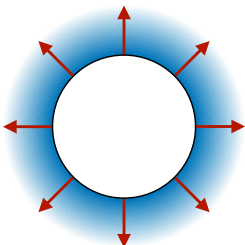
$$\Gamma \propto e^{-\frac{S_3(T)}{T}} = e^{\beta(t-t_0)} \implies \frac{\beta}{H} = T \frac{d}{dT} \left(\frac{S_3(T)}{T} \right) \Big|_{T=T_*} = \frac{(8\pi)^{\frac{1}{3}}}{HR_*}$$

- Bubble wall velocity: v_w

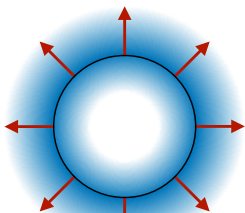


Expansion of bubbles

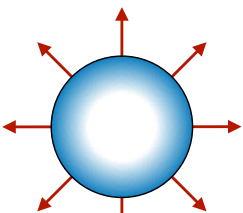
deflagration $v_w < c_s$



hybrid $c_s < v_w < c_J$



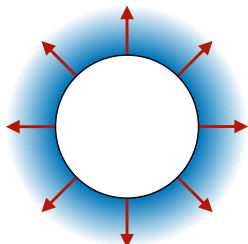
detonation $c_J < v_w$



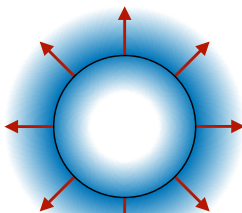
with speed of sound $c_s = \frac{1}{\sqrt{3}}$ and the Jouget velocity $c_J = \frac{1}{\sqrt{3}} \frac{1+\sqrt{3\alpha^2+2\alpha}}{1+\alpha}$.

Expansion of bubbles

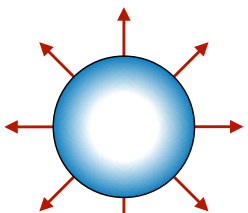
deflagration $v_w < c_s$



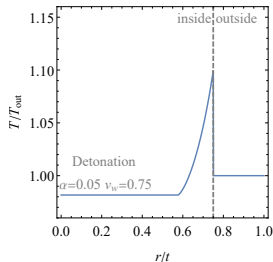
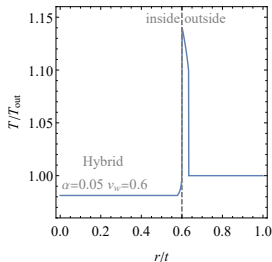
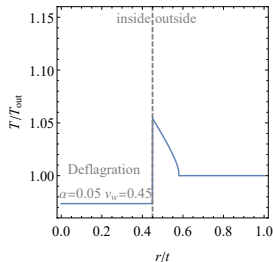
hybrid $c_s < v_w < c_J$



detonation $c_J < v_w$

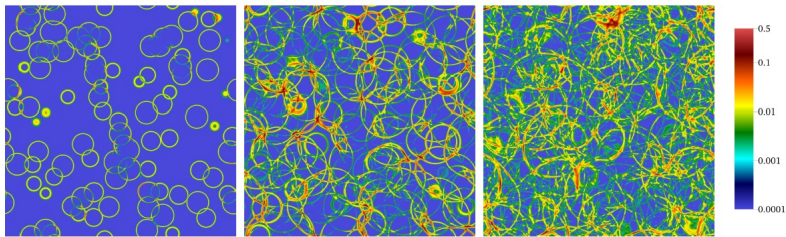


with speed of sound $c_s = \frac{1}{\sqrt{3}}$ and the Jouget velocity $c_J = \frac{1}{\sqrt{3}} \frac{1+\sqrt{3\alpha^2+2\alpha}}{1+\alpha}$.



Sound Waves

- Simulation of a scalar coupled to the plasma



- Fit to the GW spectrum

$$\Omega_{\text{gw}} \propto \left(\frac{f}{f_p}\right)^3 \left(\frac{7}{4 + 3(f/f_p)^2}\right)^{\frac{7}{2}}$$

Hindmarsh, Huber, Rummukainen, Weir, arXiv: 1504.03291, 1704.05871

- Sound shell model

arXiv: 1608.04735 1909.10040, 2106.05984, 2308.12916, 2308.12943

Sound Waves

- Higgsless simulation of the plasma

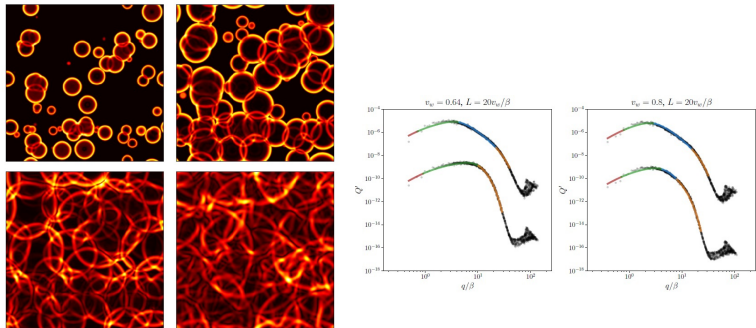
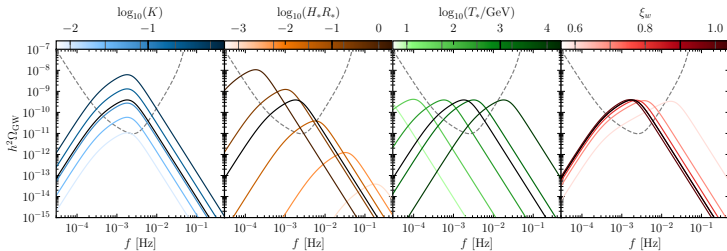


Figure 4: Kinetic energy v^2 in different simulation snapshots: $t = 2.7/\beta$ (top left), $5.4/\beta$ (top right), $10.8/\beta$ (bottom left) and $20.1/\beta$ (bottom right). We use box size $L = 40v_w/\beta$, weak transitions and $v_w = 0.8$.

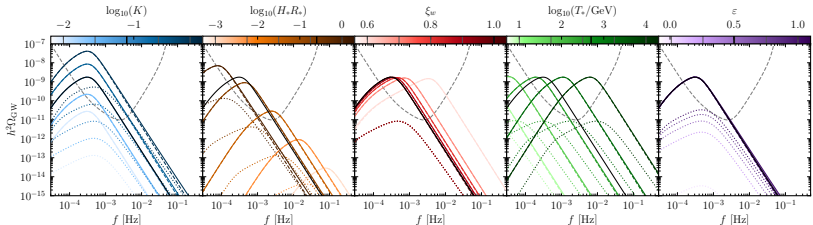
- Fit to the GW spectrum

$$\Omega_{\text{gw}} \propto \frac{(f/f_1)^3}{1 + (f/f_1)^2[1 + (f/f_2)^4]}, \quad f_2/f_1 \approx 1/\xi_{\text{shell}}$$

- sound waves



- sound waves (solid) + turbulence (dotted)



Dynamics of the steady state expansion

Integrated EoM of the growing bubble:

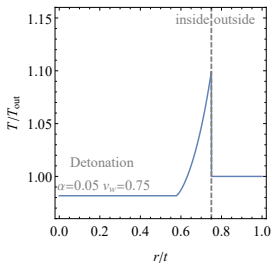
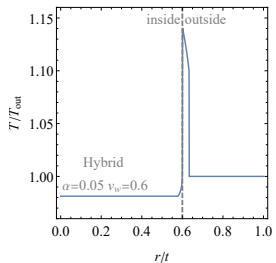
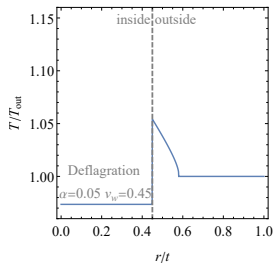
$$\int dz \frac{d\phi}{dz} \left(\square\phi + \frac{\partial V_{\text{eff}}}{\partial \phi} + \sum_i \frac{dm_i^2(\phi)}{d\phi} \int \frac{d^3 p}{(2\pi)^3 2E_i} \delta f_i(p, x) \right) = 0$$

$$\downarrow \frac{d\phi}{dz} \frac{\partial V_{\text{eff}}}{\partial \phi} = \frac{dV_{\text{eff}}}{dz} - \frac{\partial V_{\text{eff}}}{\partial T} \frac{dT}{dz}$$

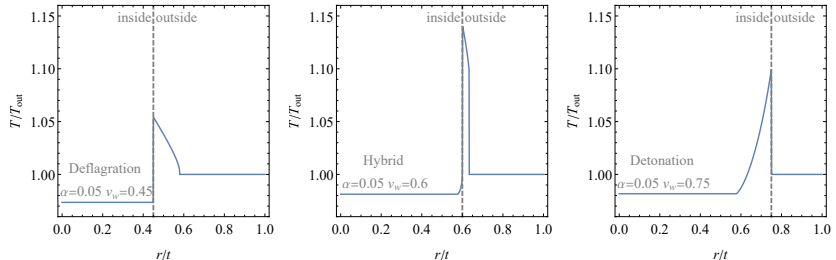
$$\Delta V_{\text{eff}} = \boxed{\int dz \frac{\partial V_{\text{eff}}}{\partial T} \frac{dT}{dz}} - \boxed{\sum_i \int d\phi \frac{dm_i^2(\phi)}{d\phi} \int \frac{d^3 p}{(2\pi)^3 2E_i} \delta f_i(p, x)}$$

driving force = hydrodynamic backreaction + non-equilibrium friction

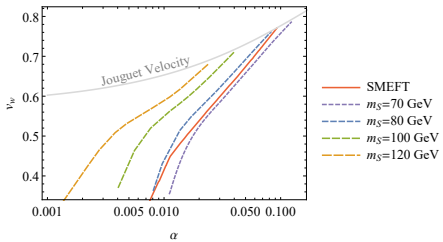
Wall Velocity



Wall Velocity



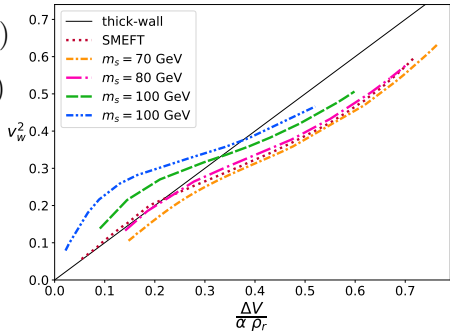
- No solutions found beyond $c_J = \frac{1}{\sqrt{3}} \frac{1 + \sqrt{3\alpha^2 + 2\alpha}}{1 + \alpha}$.



Wall Velocity analytic approximation

$$v_w = \begin{cases} \sqrt{\frac{\Delta V}{\alpha \rho_R}} & \text{for } \sqrt{\frac{\Delta V}{\alpha \rho_R}} < v_J(\alpha) \\ 1 & \text{for } \sqrt{\frac{\Delta V}{\alpha \rho_R}} \geq v_J(\alpha) \end{cases}$$

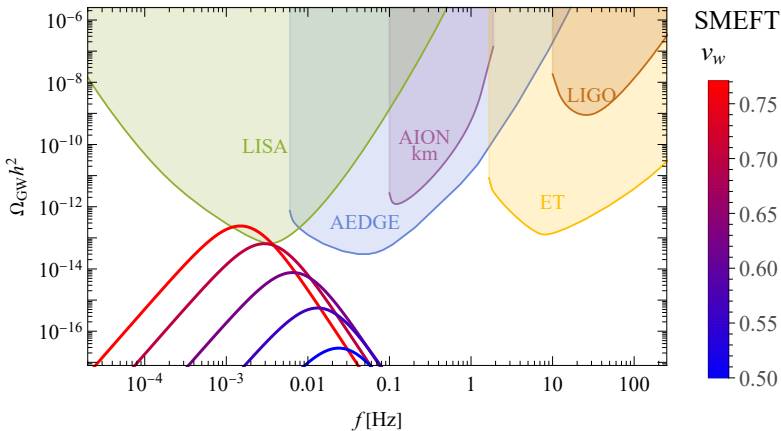
- Here: $\alpha = \frac{1}{\rho_R} \left(\Delta V - \frac{T}{4} \frac{\partial \Delta V}{\partial T} \right)$
- Formula does not require solving transport equations
- Only the form of the potential is important



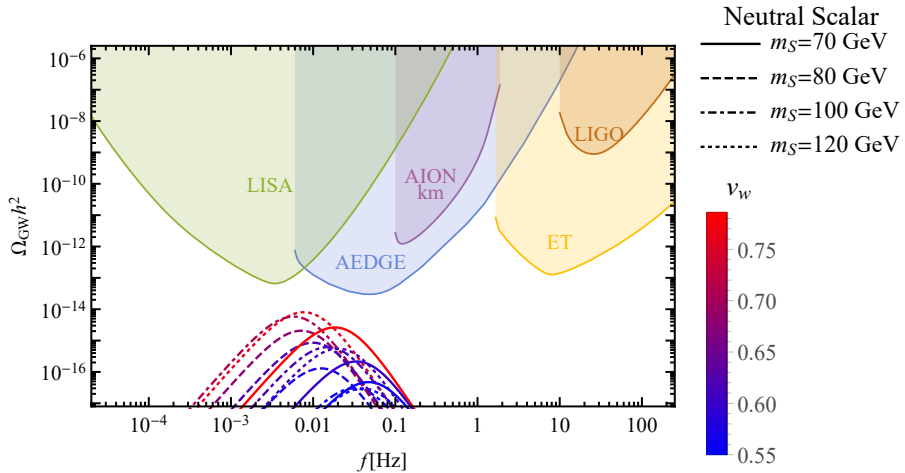
ML, Marco Merchand, Mateusz Zych, JHEP **02** (2022) 017, arXiv: 2111.02393

John Ellis, ML, Marco Merchand, José Miguel No, Mateusz Zych arXiv:2210.16305

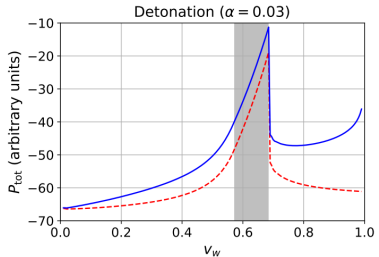
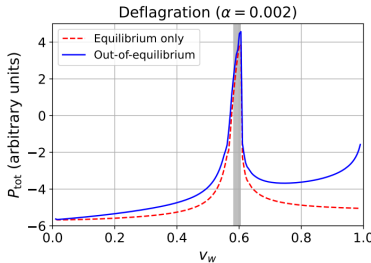
Gravitational wave signals



Gravitational wave signals



- Impact of out-of-equilibrium effects is small



Benoit Laurent, James Cline arXiv:2204.13120

- LTE approximation ($\delta f = 0$)

$$v_w = \left(\left| \frac{3\alpha + \Psi - 1}{2(2 - 3\Psi + \Psi^3)} \right|^{\frac{p}{2}} + \left| v_{\text{CJ}} \left(1 - a \frac{(1 - \Psi)^b}{\alpha} \right) \right|^{\frac{p}{2}} \right)^{\frac{1}{p}}$$

with $a = 0.2233$, $b = 1.704$, $p = -3.433$ and $\Psi = \frac{w_t}{w_f}$

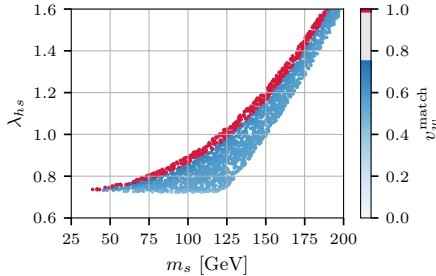
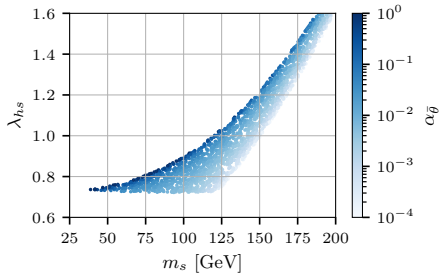
Wen-Yuan Ai, Benoit Laurent, Jorinde van de Vis arXiv:2303.10171

Scalar singlet extension

- Standard Model with an additional singlet scalar

$$V(H, s) = -\mu_h^2 |H|^2 + \lambda |H|^4 + \frac{\lambda_{hs}}{2} S^2 |H|^2 + \left(\textcolor{blue}{m_s}^2 - \frac{\lambda_{hs} v^2}{2} \right) \frac{s^2}{2} + \frac{\lambda_s}{4} S^4$$

- Scan of the parameter space with $\lambda_s = 1$.
- Wall velocity determined analytically with matching conditions assuming LTE.



Lattice realisation

- The energy-momentum tensor for the field and the fluid:

$$T_{\text{field}}^{\mu\nu} = \partial^\mu \phi \partial^\nu \phi - g^{\mu\nu} \left(\frac{1}{2} \partial_\alpha \phi \partial^\alpha \phi \right)$$
$$T_{\text{fluid}}^{\mu\nu} = w u^\mu u^\nu + g^{\mu\nu} p$$

- effective coupling of the fluid and scalar:

$$\nabla_\mu T_{\text{field}}^{\mu\nu} = -\nabla_\mu T_{\text{fluid}}^{\mu\nu} = \frac{\partial V(\phi, T)}{\partial \phi} \partial^\nu \phi + \eta u^\mu \partial_\mu \phi \partial^\nu \phi$$

- Equation of state

$$p(\phi, T) = -V(\phi, T),$$

$$e(\phi, T) = V(\phi, T) - T \frac{dV(\phi, T)}{dT},$$

$$w(\phi, T) = -T \frac{dV(\phi, T)}{dT}.$$

Lattice realisation: EoM

- EoM for scalar fields assuming **LTE** $\eta = 0$

$$\begin{aligned}-\partial_t^2 h + \frac{1}{r^2} \partial_r (r^2 \partial_r h) - \frac{\partial V}{\partial h} &= 0 \\-\partial_t^2 s + \frac{1}{r^2} \partial_r (r^2 \partial_r s) - \frac{\partial V}{\partial s} &= 0\end{aligned}$$

Lattice realisation: EoM

- EoM for scalar fields assuming **LTE** $\eta = 0$

$$\begin{aligned}-\partial_t^2 h + \frac{1}{r^2} \partial_r(r^2 \partial_r h) - \frac{\partial V}{\partial h} &= 0 \\-\partial_t^2 s + \frac{1}{r^2} \partial_r(r^2 \partial_r s) - \frac{\partial V}{\partial s} &= 0\end{aligned}$$

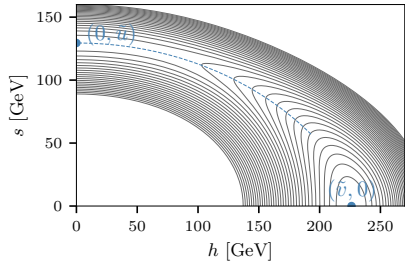
- EoM for plasma assuming **LTE** $\eta = 0$

$$\begin{aligned}\partial_t \tau + \frac{1}{r^2} \partial_r(r^2(\tau + p)v) &= \frac{\partial V_{\text{eff}}}{\partial h} \partial_t h + \frac{\partial V_{\text{eff}}}{\partial s} \partial_t s \\ \partial_t Z + \frac{1}{r^2} \partial_r(r^2 Z v) + \partial_r p &= -\frac{\partial V_{\text{eff}}}{\partial h} \partial_r h - \frac{\partial V_{\text{eff}}}{\partial s} \partial_r s\end{aligned}$$

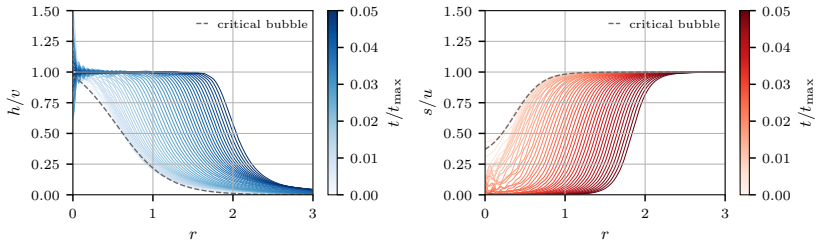
where $Z := w\gamma^2 v$ and $\tau := w\gamma^2 - p$

Evolution: early stages

- Initial $h(r)$ and $s(r)$ profiles corresponding to the critical bubble.

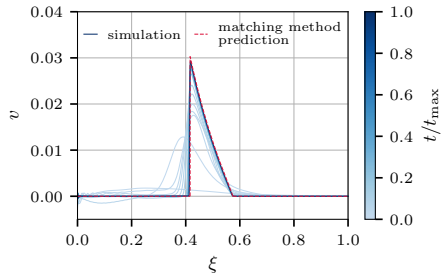


- Plasma initially at rest $v(r) = 0$ with nucleation temperature $T(r) = T_n$



Evolution: late stages

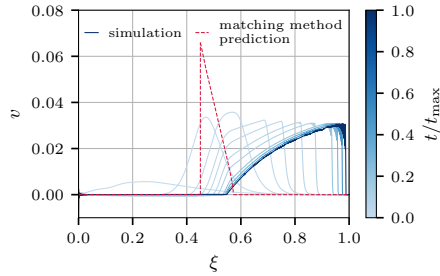
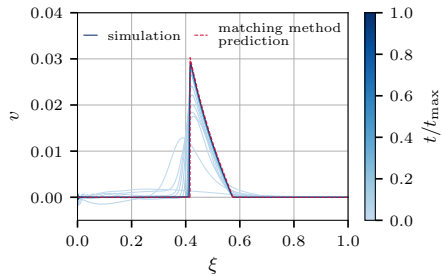
- Self-similar profiles: $\xi = r/t$
- Two possible scenarios for the growing bubble in LTE:



- evolution toward a stationary state predicted by matching conditions

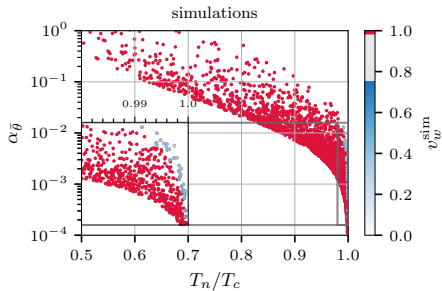
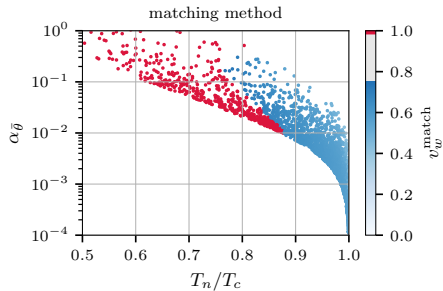
Evolution: late stages

- Self-similar profiles: $\xi = r/t$
- Two possible scenarios for the growing bubble in LTE:



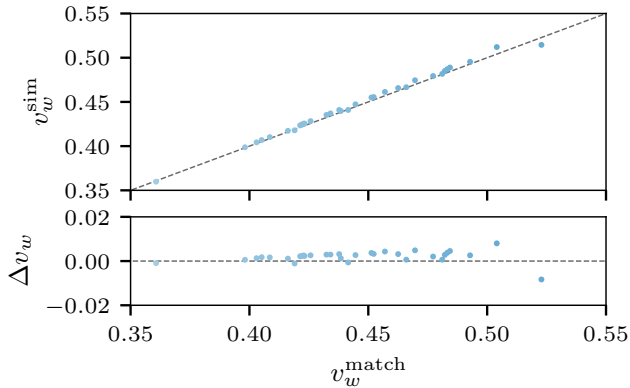
- evolution toward a stationary state predicted by matching conditions
- rapid expansion beyond Chapman-Jouguet velocity leading to a runaway scenario

Analytical treatment vs real-time simulations



- Matching equations predict significant number of stationary deflagrations and hybrids.
- Real-time simulations predict only a few points evolve towards a stationary state.

Analytical treatment vs real-time simulations



If the stationary state is achieved for a given model, bubble-wall velocity is very accurately predicted by the matching equations.

Conclusions

- GW within the reach of upcoming experiments are typically produced in transitions with very relativistic wall velocities $v_w \approx 1$. This produces a tension with electroweak baryogenesis which requires slower walls.
- Lattice simulations in the absence of non-equilibrium friction predict bubbles to generically expand as runaways even in cases where matching conditions predict a slower wall.
- Stationary profiles are dynamically achieved only for tiny supercooling ($T_n/T_c \lesssim 1$).

Conclusions

- GW within the reach of upcoming experiments are typically produced in transitions with very relativistic wall velocities $v_w \approx 1$. This produces a tension with electroweak baryogenesis which requires slower walls.
- Lattice simulations in the absence of non-equilibrium friction predict bubbles to generically expand as runaways even in cases where matching conditions predict a slower wall.
- Stationary profiles are dynamically achieved only for tiny supercooling ($T_n/T_c \lesssim 1$).

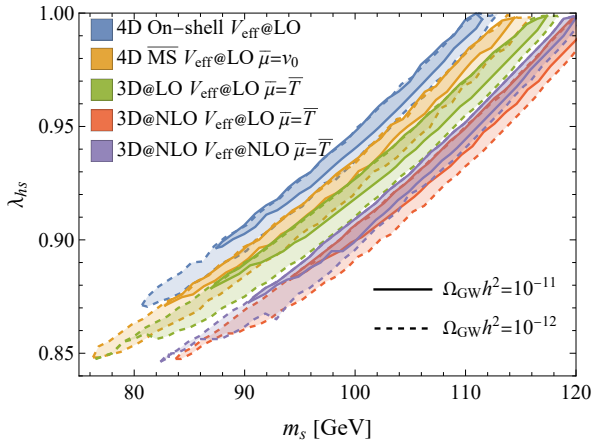
Thank you for your attention!

Backup Slides

Theoretical uncertainty on the parameter space

- Standard Model with an additional singlet scalar

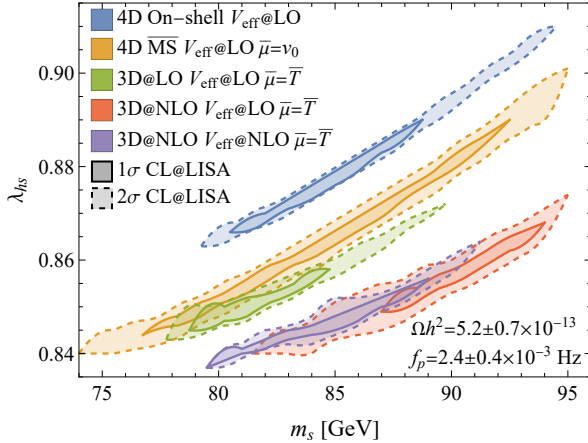
$$V(H, s) = -\mu_h^2 |H|^2 + \lambda |H|^4 + \frac{\lambda_{hs}}{2} S^2 |H|^2 + \left(m_s^2 - \frac{\lambda_{hs} v^2}{2} \right) \frac{s^2}{2} + \frac{\lambda_s}{4} S^4$$



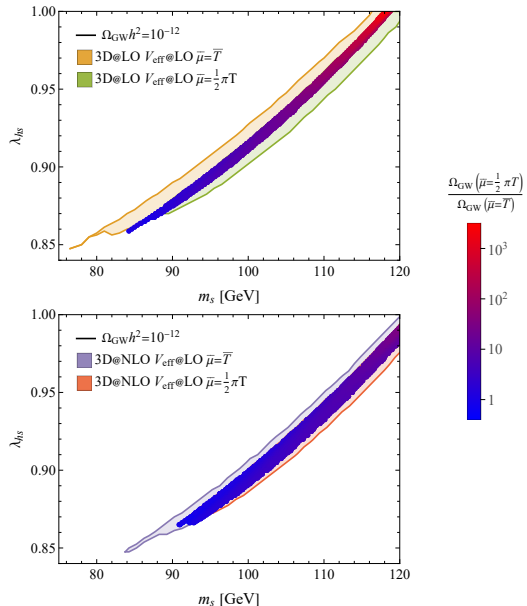
Theoretical uncertainty on the parameter reconstruction

- Standard Model with an additional singlet scalar

$$V(H, s) = -\mu_h^2 |H|^2 + \lambda |H|^4 + \frac{\lambda_{hs}}{2} S^2 |H|^2 + \left(m_s^2 - \frac{\lambda_{hs} v^2}{2} \right) \frac{s^2}{2} + \frac{\lambda_s}{4} S^4$$

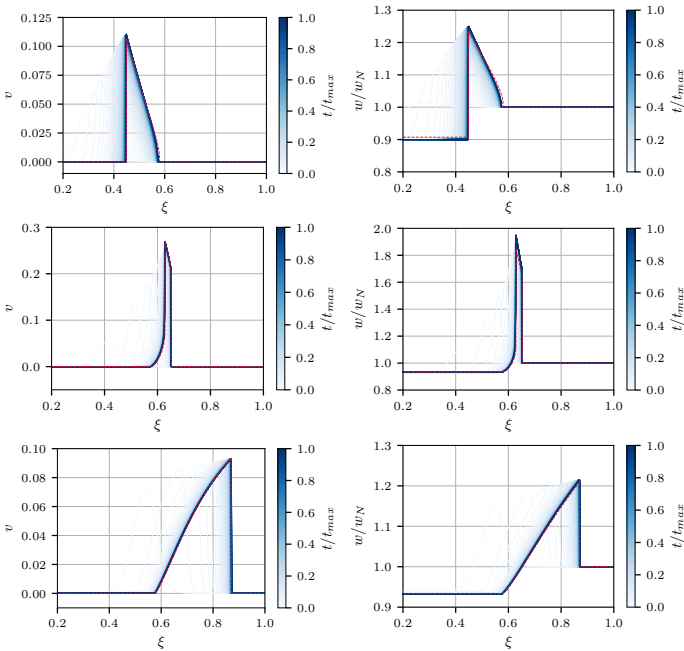


Theoretical uncertainty on the parameter space

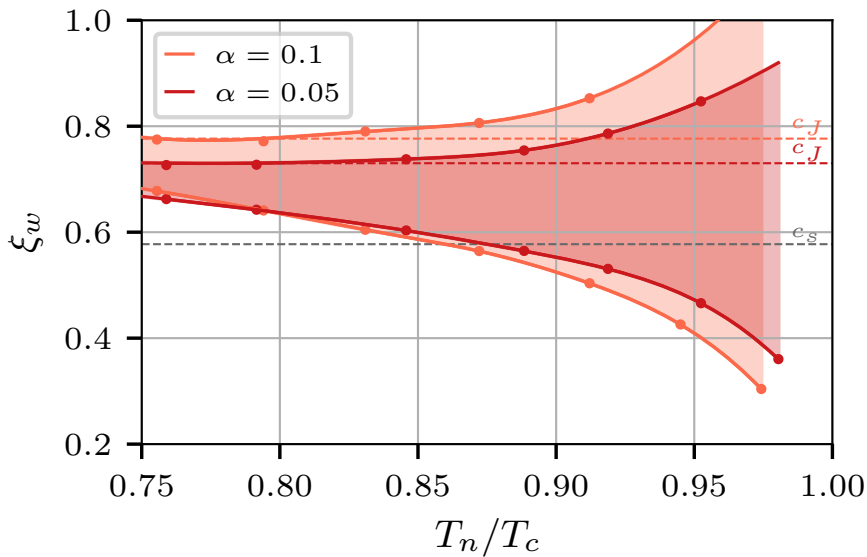


Conclusions II

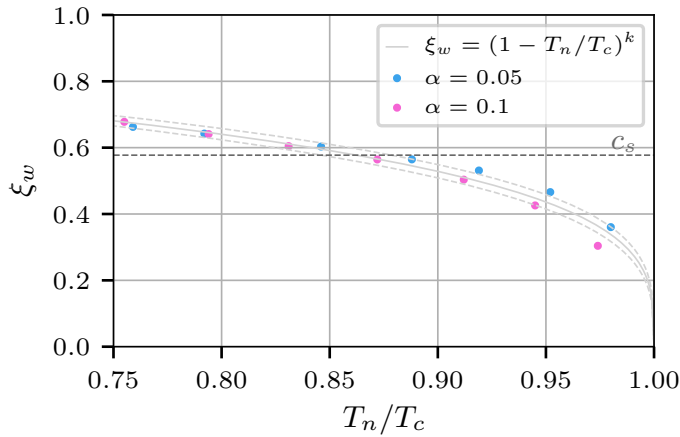
- Large errors on the GW spectra for individual parameter points corresponds to small $O(1\%)$ error on the reconstructed model parameters
- These small reconstruction errors would still dominate the experimental uncertainties for any detectable spectra



Hydrodynamical obstruction: can all v_w be realised?



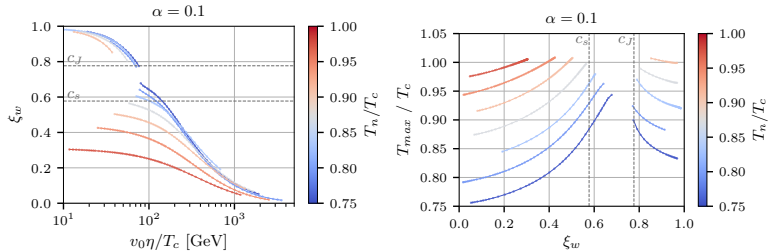
Hydrodynamical obstruction: numerical fit



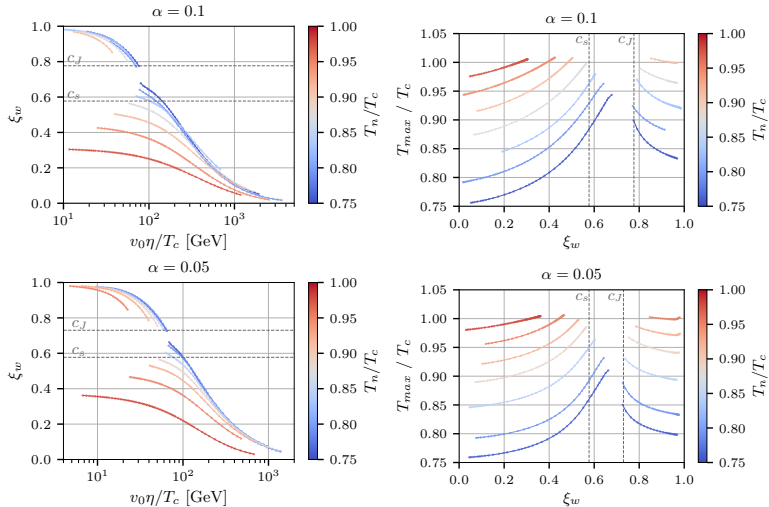
- Simple numerical fit accurate for relatively strong PTs

$$v_w = \left(1 - \frac{T_n}{T_c}\right)^k, \quad \text{with} \quad k = 0.2768 \pm 0.0055$$

Hydrodynamical obstruction: numerical fit

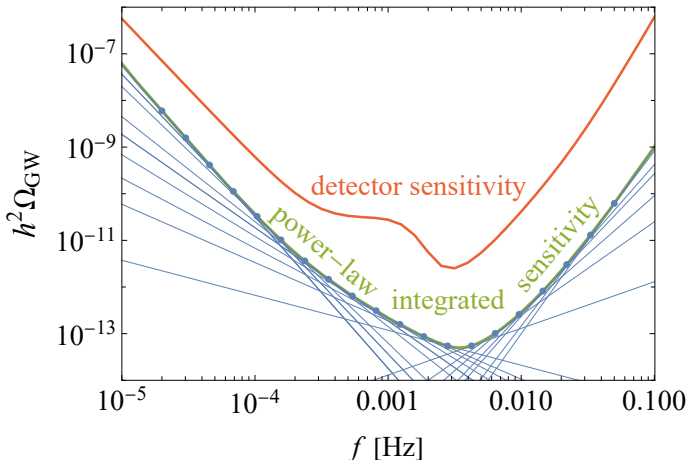


Hydrodynamical obstruction: numerical fit

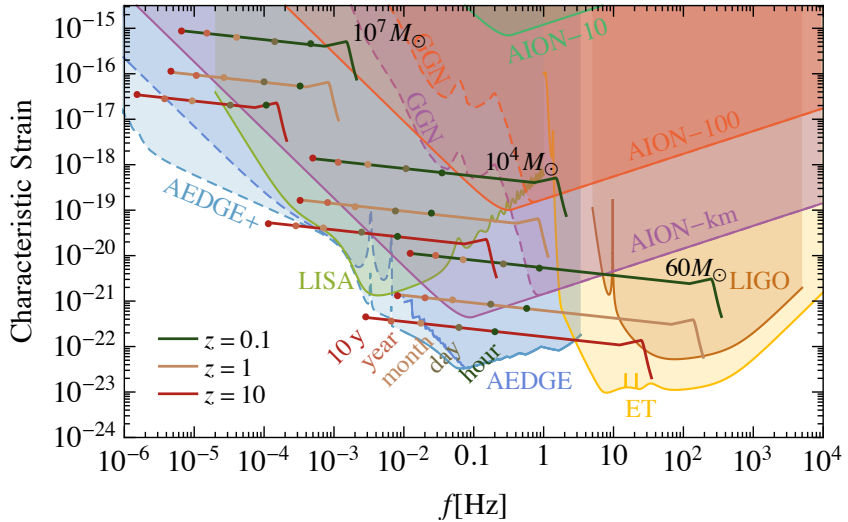


Power-law integrated sensitivity

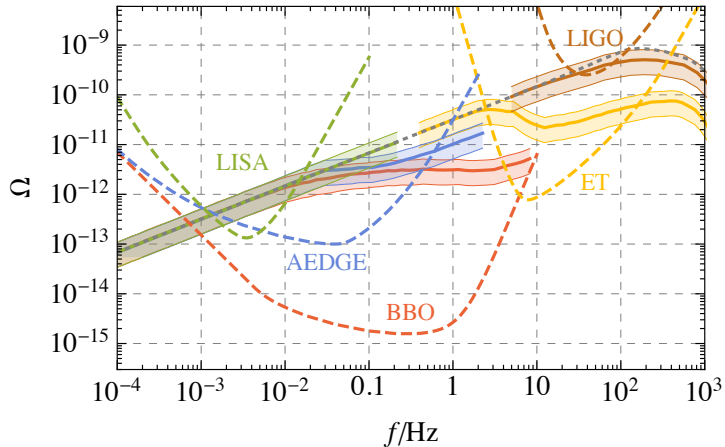
$$\Omega_{\text{GW}}^{\text{noise}} = \frac{2\pi}{3} \frac{f^3 h_c^2}{H_0^2}, \quad \text{SNR} = \sqrt{\mathcal{T} \int df \left(\frac{\Omega_{\text{GW}}^{\text{signal}}}{\Omega_{\text{GW}}^{\text{noise}}} \right)^2}, \quad \Omega_{\text{GW}}^{\text{signal}} = \Omega \left(\frac{f}{f_{\text{ref}}} \right)^\alpha$$



Sensitivity to binary mergers



Foreground from LIGO-Virgo binaries

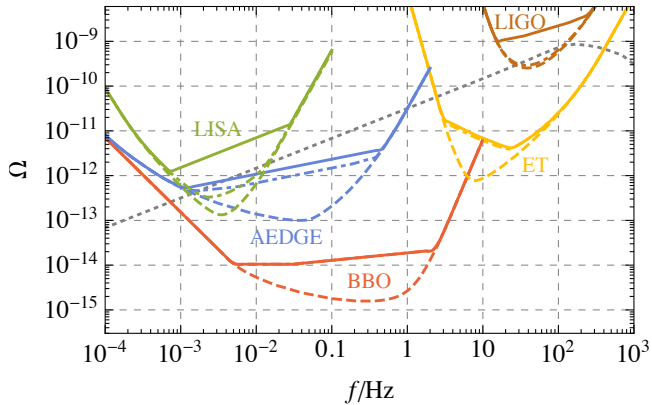


- Dashed gray line: total foreground from LIGO-Virgo binaries
- Thick lines: foreground without individually observable binaries

Improved sensitivities from Fisher analysis

- assuming power-law signal as in PI sensitivity

$$\Omega_{\text{GW}}(f) = \Omega \left(\frac{f}{f_{\text{ref}}} \right)^{\alpha} + A \langle \Omega_{\text{BBH}}(f) \rangle + \Omega_{\text{BWD}}(f) + \Omega_{\text{instr}}(f)$$



Above the Jouguet velocity. Can the walls run away?

- Energy of the bubble

$$\mathcal{E} = 4\pi \textcolor{blue}{R}^2 \sigma \textcolor{green}{\gamma} - \frac{4\pi}{3} \textcolor{blue}{R}^3 p, \quad \textcolor{green}{\gamma} = \frac{1}{\sqrt{1 - \dot{\textcolor{blue}{R}}^2}}$$

- Vacuum pressure on the wall

Coleman '73

$$p_0 = \Delta V$$

Above the Jouguet velocity. Can the walls run away?

- Energy of the bubble

$$\mathcal{E} = 4\pi \textcolor{blue}{R}^2 \sigma \textcolor{green}{\gamma} - \frac{4\pi}{3} \textcolor{blue}{R}^3 p, \quad \textcolor{green}{\gamma} = \frac{1}{\sqrt{1 - \dot{\textcolor{blue}{R}}^2}}$$

- Vacuum pressure on the wall

Coleman '73

$$p_0 = \Delta V$$

- Leading order plasma contribution

Bodeker '09 Caprini '09

$$p_1 = \Delta V - \Delta P_{\text{LO}} \approx \Delta V - \frac{\Delta m^2 \textcolor{red}{T}^2}{24},$$

Above the Jouguet velocity. Can the walls run away?

- Energy of the bubble

$$\mathcal{E} = 4\pi \textcolor{blue}{R}^2 \sigma \gamma - \frac{4\pi}{3} \textcolor{blue}{R}^3 p, \quad \gamma = \frac{1}{\sqrt{1 - \dot{\textcolor{blue}{R}}^2}}$$

- Vacuum pressure on the wall

Coleman '73

$$p_0 = \Delta V$$

- Leading order plasma contribution

Bodeker '09 Caprini '09

$$p_1 = \Delta V - \Delta P_{\text{LO}} \approx \Delta V - \frac{\Delta m^2 \textcolor{red}{T}^2}{24},$$

- Next-To-Leading order plasma contribution

Bodeker '17 Goutteneoire '21

$$p = \Delta V - \Delta P_{\text{LO}} - \gamma \Delta P_{\text{NLO}} \approx \Delta V - \frac{\Delta m^2 \textcolor{red}{T}^2}{24} - \gamma g^2 \Delta m_V \textcolor{red}{T}^3.$$

- Next-To-Leading order plasma contribution with resummation

Hoche '20

$$P = \Delta V - P_{1 \rightarrow 1} - \gamma^2 P_{1 \rightarrow N} \approx \Delta V - 0.04 \Delta m^2 \textcolor{red}{T}^2 - 0.005 g^2 \gamma^2 \textcolor{red}{T}^4.$$